CRYSTAL GROWTH & DESIGN

Article

pubs.acs.org/crystal

Coordination-Induced Assembly of Coordination Polymer Submicrospheres: Promising Antibacterial and in Vitro Anticancer Activities

Kuaibing Wang, Xiaoyan Ma, Dalin Shao, Zhirong Geng, Zhiyang Zhang, and Zhilin Wang*

State Key Laboratory of Coordination Chemistry, School of Chemistry and Chemical Engineering, Nanjing University, Nanjing National Laboratory of Microstructures, Nanjing 210093, People's Republic of China

Supporting Information

ABSTRACT: Spheres-like coordination polymer architectures in submicro regimes have been synthesized from the hydrothermal reaction of transition metal ions and 3,5-bis(pyridin-3-ylmethylamino)benzoic acid (L1). The size of the final coordination polymer was dependent on the concentrations of reactants. Scanning electron microscopy studies monitored at numerous stages of growth reveal that coordination-induced morphology changes from uncoordinated flowerlike ligands to sphere-like coordination polymer particles. Moreover, variations of luminescent and antibacterial profiles are associated with coordination environments or the size of as-obtained coordination polymer samples. In addition, the newly synthesized Cu-based polymer particles may act as novel metal-based anticancer drugs in the future because of their potent in vitro anticancer activities against three chosen cancer lines MCF-7, HeLa, and NCI-H446.

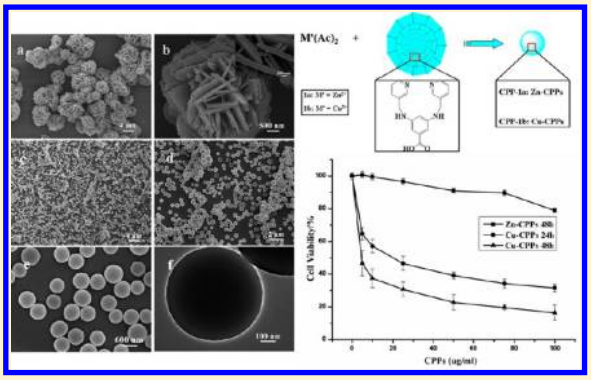

INTRODUCTION

Micrometer- and submicrometer-sized colloids have been successfully applied in numerous fields, such as biosensors[1] and porous membranes[2] and hold promise as decomposable templates for the fabrication of hollow spheres,[3] etc. Particularly, coordination polymer particles (CPPs) are now being designed into a new class of colloidal materials not only due to their unique applications in gas storage,[4] optics,[5] and drug delivery[6] but also because of the incorporation of coordination polymers with other solid materials that produces hybrid materials and generates metal oxides as precursors.[7,8] Multifunctional organic or organometallic ligand building blocks have been used to synthesize infinite CPPs, but the preparations of micro- or nanomaterials have less been reported[9,10] and are commonly ignored by many researchers in the fabrication of CPPs. Thus, the morphology of the organic linker itself may play a vital role in building size- and morphology-dependent multifunctional CPPs.

To date, much efforts have been devoted to the design and preparation of transition metal coordination polymer materials because these metals are physiologically essential metal elements that function in endogenous oxidative DNA damage associated with aging and cancer.[11] Metal ions that are essential for cells may become toxic at high concentrations because they can replace other important metals in enzymes.[12] Accordingly, lots of literature has focused on coordination compounds materials because of their good biocompatibility.[13] Besides, coordination polymers can interact with DNA through noncovalent interactions, including intercalation and groove binding for large molecules and slot external electrostatic binding for cations. It has been previously reported that Cu-based complexes showed promising antineoplastic activity against cancer cells in vitro.[14]

It is noteworthy that the recently recognized structures of well-designed coordination polymer materials include crystalline metal−organic frameworks (MOFs)[15,16] and amorphous CPPs.[17] However, none of these reports have referred their anticancer activities as a function of micro/nanoscale architectures. Indeed, it has been proven that spherelike CPPs are effective in drug delivery systems.[6a,18,19] In our previous work, we also found the interesting antimicrobial activities of micro/nanosized CPPs as a function of morphology.[20] Therefore, we aim to utilize CPPs as potential anticancer drugs in the form of submicroscale spherical particles. Herein, anticancer activities of the as-prepared CPPs and freshly synthesized N-containing linker were investigated under identical experimental conditions. Besides, the antibacterial profiles were also studied to explore the bioactivities of CPPs. Furthermore, the process and the mechanism of assembling flowerlike organic building blocks into biofunctional spherical particles were also documented.

Received: May 7, 2012
Revised: June 4, 2012
Published: June 7, 2012

   dx.doi.org/10.1021/cg3006162 | *Cryst. Growth Des.* 2012, 12, 3786−3791

EXPERIMENTAL SECTION

Materials and Measurements. Elemental analyses of C, H, and N were performed on an Elementar Vario Micro Elemental Analyzer at the Analysis Centre of Nanjing University. Fourier-transformed infrared (FT-IR) spectra were obtained on a Bruker Vector 22 FT-IR spectrophotometer using KBr pellets. X-ray powder diffraction (XRPD) data were collected on a Bruker D8 Advance instrument using Cu Kα radiation (λ = 1.54056A °) at room temperature. The morphology of the as-prepared samples and the corresponding energy dispersive X-ray (EDX) spectroscopy were obtained by a Hitachi S-4800 field-emission scanning electron microscope (FE-SEM). Transmission electron microscopy (TEM) images were captured on the JEM-2100 instrument microscopy at an acceleration voltage of 200 kV. The adsorption isotherm of nitrogen was measured at 77 K by using Micromeritics ASAP 2020 M+C volumetric adsorption equipment. ESI-MS measurements were performed with an LCQ fleet mass spectrometer. ^{1}H and ^{13}C NMR (TMS used as internal standard) spectra were recorded with a Bruker ARX 300 spectrometer, and $CDCl_3$ was used as the solvent.

Synthesis of Zn-CPPs (CPP-1a). A mixture of $Zn(Ac)_2$ (0.011 g) and L1 (0.017 g) with a molar ratio of about 1:1 in 20 mL of H_2O was placed in a 50 mL Teflon-lined stainless steel autoclave, which was sealed and heated to 140 °C for 1 h. The solid material was collected by centrifugation and washed with water and CH_3CH_2OH for several times. IR for **1** (KBr pellet, cm^{-1}): 1607 (s), 1532 (s), 1406 (s), 1322 (m), 1187 (m), 1027 (s), 950 (w), 860 (w), 786 (w), 701 (w), 664 (w) and 508 (w). Anal. calcd for CPP-**1a** $[Zn(L1)(OH)(H_2O)_2]_n$: C, 50.55; H, 4.42; N, 12.42%. Found: C, 50.48; H, 4.39; N, 12.22%.

Synthesis of Cu-CPPs (CPP-1b). An identical procedure for CPP-**1a** was followed to prepare CPP-**1b** except that $Zn(Ac)_2$ was replaced by $Cu(Ac)_2$. IR for **1** (KBr pellet, cm^{-1}): 1607 (s), 1555 (s), 1397 (s), 1321 (m), 1193 (m), 1028 (w), 948 (w), 861 (w), 797 (w), 704 (w), 657 (w) and 502(w). Anal. calcd for CPP-**1a** $[Cu(L1)(OH)(H_2O)_2]_n$: C, 50.71; H, 4.45; N, 12.46%. Found: C, 50.94; H, 4.72; N, 12.48%. There are inherent difficulties in determining CPP's exact inner structure due to the limitations of X-ray diffraction; however, the formula of $[M(L1)(OH)(H_2O)_2]_n$ (M = Zn or Cu) was deduced from the analysis of EA data, and this result is consistent with EDX data.

Antibacterial Test. Antibacterial activities of the synthesized CPPs were tested against *B. subtilis*, *S. aureus*, *S. faecalis*, *P. aeruginosa*, and *E. cloacae* by determining the minimum inhibitory concentrations (MICs, μg mL^{-1}) through a colorimetric method using the dye MTT [3-(4,5-dimethylthiazol-2-yl)-2,5-diphenyltetrazolium bromide]. First, stock solutions of the synthesized samples (50 μg/mL) were prepared in dimethyl sulfoxide (DMSO), and graded quantities of the test crystals were incorporated in a specified quantity of sterilized liquid medium. Second, the solutions were poured into microtitration plates, to which was then added approximately 10^5 cfu/mL suspension of the microorganism. After incubation at 37 °C for 24 h, 50 μL of PBS (phosphate-buffered saline, 0.01 mol/L, pH 7.4: $Na_2HPO_4{\cdot}12H_2O$, 2.9 g; KH_2PO_4, 0.2 g; NaCl, 8.0 g; KCl, 0.2 g; and distilled water, 1000 mL) containing 2 mg/mL MTT was added to each well. The incubation was continued at room temperature for 4−5 h, which was followed by dye extraction by adding 100 μL of isopropanol containing 5% 1 mol/L HCl. At last, the optical density (OD) was measured with a microplate reader at 570 nm to determine the MICs.

Cell Viability Assays. A 3 × 10^4 amount of cancer cells (MCF-7, HeLa, and NCI-H446) per well was seeded in 96-well plates (TPP, St. Louis, MO) in a complete medium and kept at 37 °C in a humidified atmosphere of 5% CO_2 and incubated for 12 h prior to experimental treatments. Then, the cells were treated with various concentrations of CPP-**1a**, CPP-**1b**, L1, and solely 0.5% DMSO/H_2O solution for 24 and 48 h, respectively. Then, the culture medium was removed and refreshed with 200 μL of fresh complete medium containing 20 μL of MTT (5 mg/mL in PBS) for further 4 h of incubation. After the supernatant was removed, 150 μL/well of DMSO was added to dissolve the purple formazan crystals. The absorbance was read on a Thermo Scientific Varioskan Flash at 570 nm. Nontreated cells (in DMEM) were used as the control, and the relative cell viability (mean % ± SD, n = 3) was expressed as OD sample/OD control × 100%.

RESULTS AND DISCUSSION

In a typical experiment, N-containing lobsterlike ligand L1 was synthesized by reacting the corresponding 3,5-diaminobenzoic acid with nicotinaldehyde according to literature procedures (Scheme S1 in the Supporting Information).[21] L1 was introduced into 30 mL of water and ethanol (v:v, 1:1) under vigorous stirring at room temperature to obtain flowerlike microstructures. Then, the flowerlike ligand L1 was metalated with $Zn(Ac)_2$ or $Cu(Ac)_2$ under hydrothermal condition (Scheme 1), and the colloidal particles of Zn-based CPPs

Scheme 1. Preparation of Spherical Particles from Flowerlike Organic Building Blocks

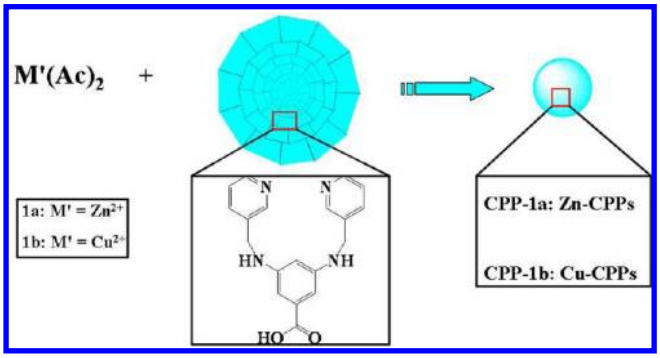

(CPP-**1a**) or Cu-based CPPs (CPP-**1b**) thus formed were collected by centrifugation, washed by absolute water and ethanol, and then suspended in ethanol for further characterization.

The flowerlike ligand L1 and amorphous (Figure S1 in the Supporting Information) spherical particles were characterized by the field-emission scanning electron microscopy (SEM) as well as a variety of other analytical techniques. As shown in Figure 1a, the average dimensions of the flowerlike ligand are 8.24 ± 0.28 μm. Figure 1b displays a higher magnified SEM image, which indicates that each flower is well-organized consisting of many nanosheets, and the width of the nanosheets is about 300 nm. In the experimental process, a 1:1 ratio of L1 linker and $Zn(Ac)_2$ [or $Cu(Ac)_2$] was used to synthesize CPP-**1a** (or CPP-**1b**) coordination polymer submicrospheres. Because of the approximate morphology, as CPP-**1a**, for example, the average dimensions of CPP-**1a** spherical particles are approximately 550 ± 100 nm as depicted in Figure 1c−e (SEM images of CPP-**1b** are shown in Figure S2 in the Supporting Information). Unfortunately, the resulting particles are not hollow spheres, which can be verified by the TEM image (Figure 1d) and N_2 adsorption isotherm (Figure S3 in the Supporting Information). The BET and Langmuir surface areas of CPP-**1a** were 4.94 and 7.34 m^2 g^{-1}, respectively. The N_2 adsorption capacity of CPP-**1a** was lower than that reported previously.[22] The chemical compositions of CPP-**1a** and CPP-**1b** were characterized by infrared spectroscopy (IR), energy-dispersive X-ray (EDX) spectroscopy (Figure S4 in the Supporting Information), and elemental analysis (EA). The stretching frequency of CO at 1689 cm^{-1} representing the uncoordinated L1 shifts to around 1607 cm^{-1}, which suggests the complete deprotonation of carboxylate group after the formation of coordination compounds. In addition, EDX confirms that the resulting samples comprise Zn (or Cu), C,

dx.doi.org/10.1021/cg3006162 | Cryst. Growth Des. 2012, 12, 3786−3791

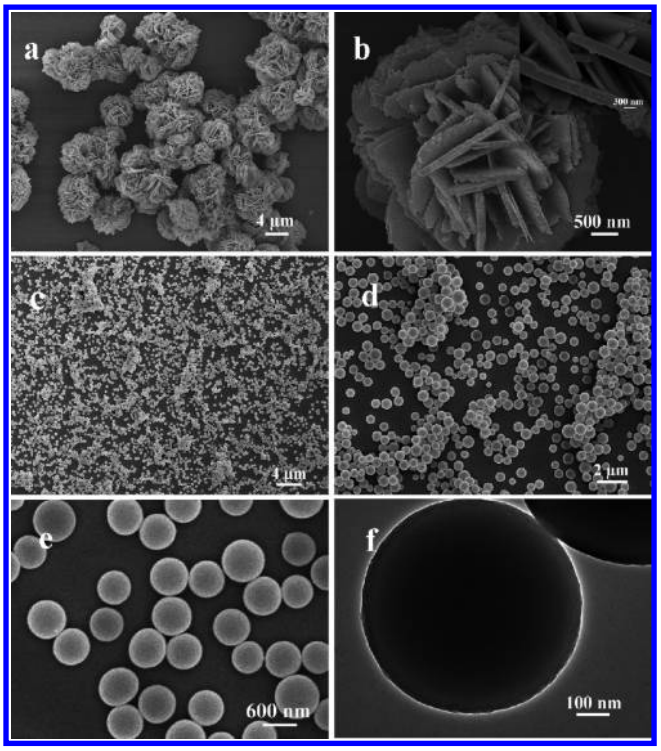

Figure 1. (a and b) SEM images of organic linker microflowers. (c and e) SEM images of sphere morphology. (f) TEM image of sphere morphology.

N, and O, and the C/N ratio is approximately 4, which is in agreement with those of EA.

To further clarify the formation procedure of these spherical particles, we tracked the transformation from organic linker to particles at different reaction times (0, 10, 20, 40, 50, and 60 min, respectively) while keeping other experimental conditions unchanged. These reactions were monitored by SEM as obviously described in Figure 2. The organic linker was flowerlike before the addition of metal ions (Figure 2a).

Initially, nanosized globular seeds and irregular rodlike oligomers are observed simultaneously (10 min, Figure 2b). As the reaction continues, the globular seeds increase significantly in the presence of crystal growth (20 min, Figure 2c). These seeds then aggregate and begin to form spherical clusters with rough surfaces (40 min, Figure 2d). Subsequently, the clusters slowly anneal into single particles after fusion (50 min, Figure 2e) and gradually form uniform particles with smoother surfaces (60 min, Figure 2f). The observations indicate that coordination interactions between the organic linker and the metal ions contribute to the transformation from microflowers to submicrospheres. Therefore, we can conclude that the formation of such submicrometer-sized spheres is attributed to the coordination-induced assembly of L1 linker and metal ions. According to the analysis of SEM images, a working mechanism concerning the formation process of spherical particles is also proposed, which includes oligomerization and nucleation, crystal growth, aggregation, fusion, and then annealing (Figure 2g). This process is similar to that of the two-step cluster-fusion mechanism in the previous literature.[5,17] Notably, physical effects probably do not dominate the polymerization process because the surfaces of seeds and particles contain many active sites for further polymerization via coordination interactions.[23,24]

We also investigated the influence of different reactant concentrations on the resulting morphology and particle size, aiming to prepare the as-synthesized samples under otherwise identical conditions. When the concentration decreased down to 1/2 of the original value, samples consisting of isolated spheres with a mean diameter of 400 nm were obtained (Figure 3a). On the other hand, increasing the concentration up to 2- and 4-fold generated spherical particles with mean diameters of 760 and 850 nm, respectively (Figure 3b,c). As shown in Figure 3c, high concentrations of reactants lead to more rough surfaces. The results reveal that the particle size generated is positively correlated with reactant concentrations significantly.

In our previous work, the coordination polymer was used in luminescence and antibacterial activity as a function of morphology. Herein, we mainly investigated whether different sizes of CPPs with the same morphology can influence

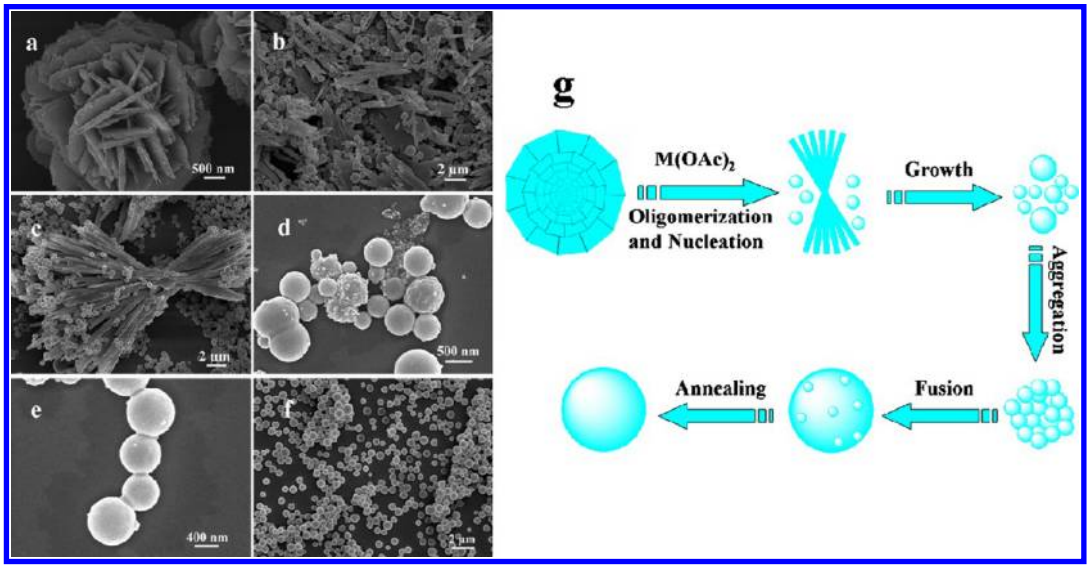

Figure 2. Representative SEM images monitoring the formation of CPPs: (a) 0, (b) 10, (c) 20, (d) 40, (e) 50, and (f) 60 min. (g) A possible model for the formation and growth of submicrospheres, which is simulated from the results of SEM.

dx.doi.org/10.1021/cg3006162 | *Cryst. Growth Des.* 2012, 12, 3786–3791

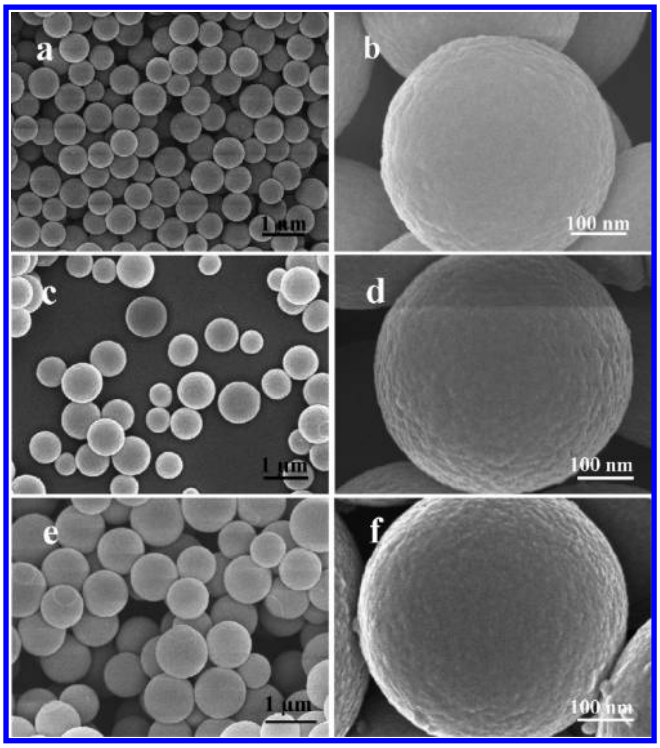

Figure 3. SEM images of spherical particles obtained with (a and b) 1/2, (c and d) 2-fold, and (e and f) 4-fold concentrations of reactants.

luminescent property and antibacterial activity. Photoluminescence properties of CPP-**1a** (mean size, 400 nm), CPP-**1b** (sample size, 400−600 nm), and L1 were studied in the solid state at room temperature upon excitation at 358 nm. As exhibited in Figure 4, L1, CPP-**1a**, and CPP-**1b** all exhibit blue

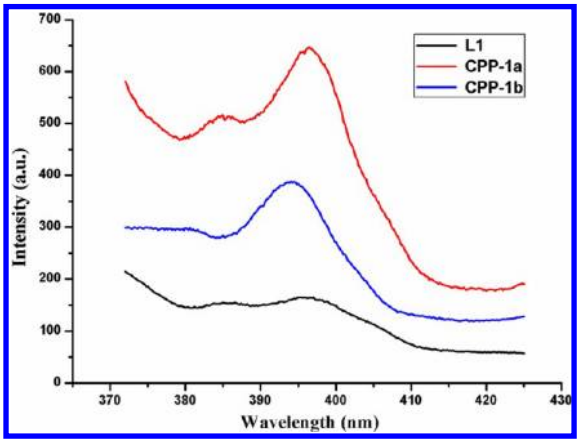

Figure 4. Fluorescence spectra of L1 linker, CPP-1a, and CPP-1b at room temperature.

luminescence emissions at ca. 396 nm. Obviously, the intensity of CPP-**1a** was higher than that of CPP-**1b**. As compared to the emission bands of the free organic linker (L1), the emissions of CPP-**1a** and CPP-**1b** may be attributable to the intraligand ($\pi-\pi^*$) transition.[25] Antibacterial activities of the synthesized CPPs against *B. subtilis*, *S. aureus*, *S. faecalis*, *P. aeruginosa*, and *E. cloacae* were tested by determining the MICs (μg mL^{-1}) through a colorimetric method using the dye MTT.[26] For comparison, the antimicrobial activities of the lobsterlike ligand were also investigated. The results summarized in Table 1 demonstrate that both CPP-**1a** and CPP-**1b** can kill *E. cloacae* well, and the flowerlike ligand does not exhibit antimicrobial activities toward the five bacteria. The as-synthesized samples are of more potent antibacterial activities in comparison with other reported Zn- or Cu-based coordination polymers.[27,28] The above observations indicate that the sample sizes with the same morphology have vital influences on the physical property and bioactivity. The different luminescent intensities reveal that the electron cloud density of oxygen atoms may change when they are coordinated to different metal ions. In addition, the different antibacterial efficacies can be ascribed to the chelation of the ligand to metal ions, thereby allowing the stronger effect of the resulting products than that of the free ligand.[27] Different antimicrobial activities toward the five bacteria of the same products may be attributed to the various structures of cell walls.[29] Moreover, the luminescent and antibacterial properties may also be affected by sample sizes.

Subsequently, the newly synthesized CPPs and the corresponding uncoordinated flowerlike ligand L1 were first evaluated for their cytotoxic activities toward breast (MCF-7) cancers. Cytotoxicity was investigated by means of MTT tests after 24 and 48 h of treatment with increasing concentrations of the tested compounds (Figure 5). CPP-**1a** and L1 are cytocompatible even after 48 h of treatment, and the cell viabilities maintain above 72 and 83% at a concentration of 100 ug/mL, which is similar to other Zn-CPPs prepared before.[20] The above result demonstrates the good biocompatibility of Zn-based CPPs. Meanwhile, CPP-**1b** leads to a dose-dependent cytotoxicity in the range of 5−100 μg/mL. IC_{50} values of CPP-**1b** obtained after 24 and 48 h of treatment in the MTT assay, calculated from the dose−viability curves, are 19.755 ± 1.217 and 4.671 ± 0.199 μg/mL, respectively.

Furthermore, in vitro antitumor activities of L1 and freshly prepared CPPs against other two cancer cell lines HeLa and NCI-H446 were conducted. As shown in Figure 6, L1 linker is compatible even after being incubated for 72 h at higher concentrations, whereas the Cu- and Zn-based compounds exhibit potent cytotoxicities against the two cancer cell lines. Therein, the IC_{50} values of Cu-based compound against HeLa and NCI-H446 after 72 h of treatment are 17.461 ± 4.943 and 30.721 ± 1.257 μg/mL, respectively. Although the underlying antitumor mechanism of CPPs is still uncertain, these results are highly significant in the following aspects: (1) Cu-based CPPs show stronger anticancer activities than Zn-based CPPs, indicating that the Cu center probably predominates in dioxygen transport, hydrolysis, and reduction of nitrogen oxides, etc. (2) In vitro antitumor activities of Cu-CPPs against MCF-7 are slightly higher than those of other Cu-based polymers,[30] which may be attributed to the interaction of CPP with the cell body or the disassociation of copper ions from CPP and the diverse coordination modes of the copper center. (3) The different cytotoxic activities of Cu-CPPs against different cancer cells under identical experimental conditions illustrate the diversities of different cancer cell lines and indicate that metal-based drugs exhibit a certain selectivity against different tumors simultaneously. Accordingly, Cu-CPPs may provide potential scientific evidence for designing novel metal-based anticancer drugs.

■ CONCLUSION

In summary, O,N-bifunctional organic ligand and 3,5-bis-(pyridin-3-ylmethylamino)benzoic acid (L1) were used for synthesizing CPPs with different metal ions with a similar

dx.doi.org/10.1021/cg3006162 | Cryst. Growth Des. 2012, 12, 3786−3791

Table 1. MICs (μg mL^{-1}) of as-Prepared CPPs and L1 Linker

	microorganisms MICs (μg/mL)				
	Gram-positive			Gram-negative	
compds	*B. subtilis*	*S. aureus*	*S. faecalis*	*P. aeruginosa*	*E. cloacae*
L1	+[a]	+	+	+	+
Zn-CPPs	>50	>50	12.5	12.5	12.5
Cu-CPPs	12.5	12.5	>50	>50	6.25
$[ZnCl_2(HATtsc)]\cdot CH_3CN$[21]	>100	>100		>100	>100
$[Cu(L)_2Cl_2]$[22]	20	24			19

[a] "+" means growth.

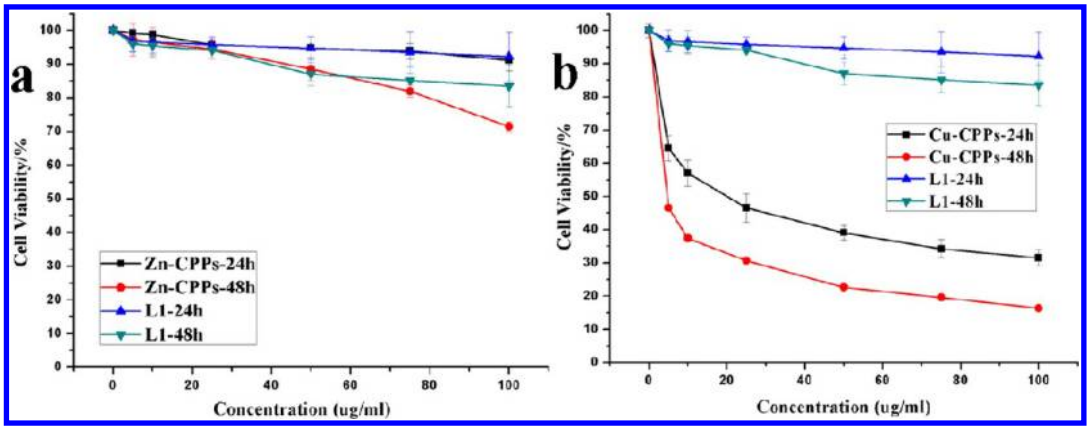

Figure 5. (a and b) Viabilities of MCF-7 cells incubated with L1 ligand and the as-synthesized samples with increasing concentrations at different time periods.

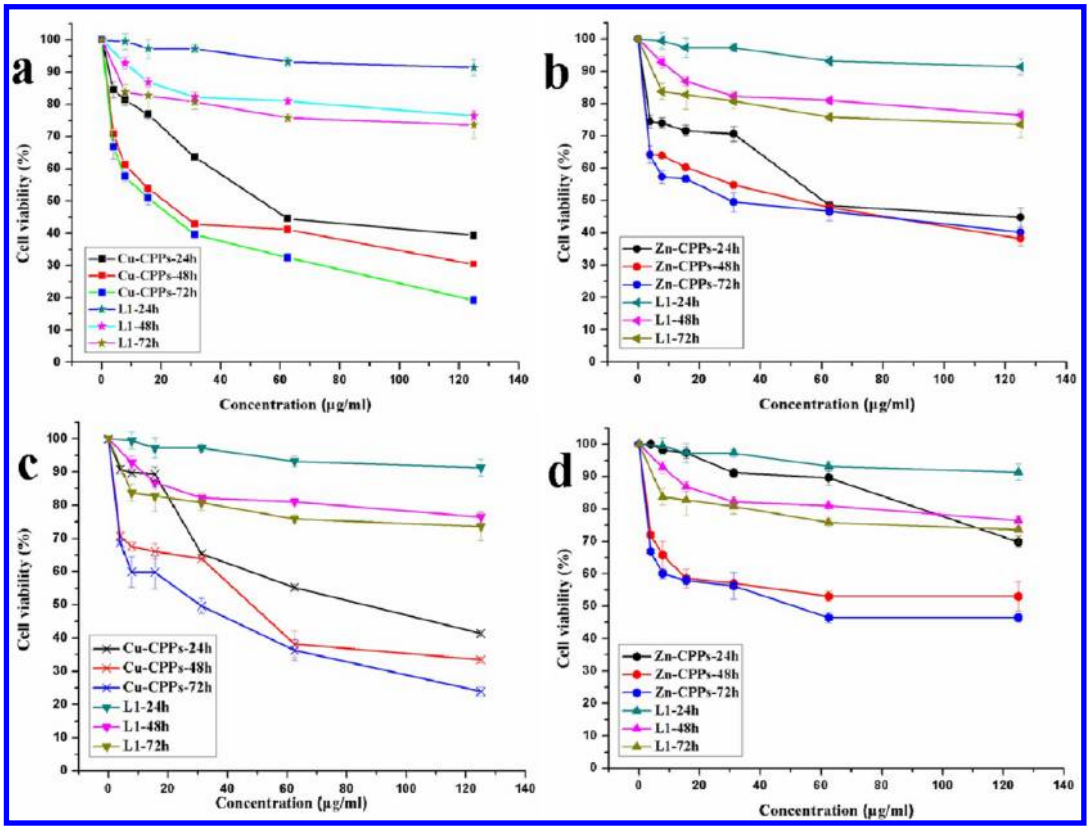

Figure 6. (a and b) Viabilities of HeLa cells and (c and d) NCI-H446 cells incubated with L1 ligand and the as-synthesized samples with increasing concentrations at different time periods.

spherelike morphology. The reaction time and reactant concentration were highly important in fabricating the resulting particles. In addition, the as-synthesized CPPs exhibited good antibacterial and photoluminescence properties, allowing them

dx.doi.org/10.1021/cg3006162 | *Cryst. Growth Des.* 2012, 12, 3786−3791

to be viable candidates for potential applications in medical and environmental fields. Furthermore, the amorphous Cu-CPPs may act as new metal-based anticancer drugs in the future due to their potent in vitro anticancer activities, high yields, and size and morphology dependences.

■ ASSOCIATED CONTENT

Supporting Information

Scheme of preparing organic building blocks, XRD patterns for CPPs, SEM images for CPP-1b, N_2 adsorption−desorption isotherms of CPP-1a, and EDX patterns and mappings for CPPs. This material is available free of charge via the Internet at http://pubs.acs.org.

■ AUTHOR INFORMATION

Corresponding Author

*Tel: +86-25-83686082. Fax: +86-25-83686082. E-mail: wangzl@nju.edu.cn.

Notes

The authors declare no competing financial interest.

■ ACKNOWLEDGMENTS

This work was supported by the National Natural Science Foundation of China (21075064, 21027013, 21021062, and 90813020) and the National Basic Research Program of China (2007CB925102).

■ REFERENCES

(1) Haes, A. J.; Hall, W. P.; Chang, L.; Klein, W. L.; Van Duyne, R. P. *Nano Lett.* **2004**, *4*, 1029−1033.
(2) Yan, F.; Goedal, W. A. *Adv. Mater.* **2004**, *16*, 911−915.
(3) Cho, W.; Lee, Y. H.; Lee, H. J.; Oh, M. *ChemComm.* **2009**, 4756−4758.
(4) (a) Tanaka, D.; Henke, A.; Albrecht, K.; Moeller, M.; Nakagawa, K.; Kitagawa, S.; Groll, J. *Nat. Chem.* **2010**, *2*, 410−416. (b) Cho, W.; Lee, H. J.; Oh, M. *J. Am. Chem. Soc.* **2008**, *130*, 16943−16946.
(5) Oh, M.; Mirkin, C. A. *Nature* **2005**, *438*, 651−654.
(6) (a) Imaz, I.; Martínez, M.-R.; Fernández, L.-G.; García, F.; Molina, D. R.; Hernando, J.; Puntes, V.; Maspoch, D. *ChemComm.* **2010**, 4737−4739. (b) Horcajada, P.; Serre, C.; Vallet-Regí, M.; Sebban, M.; Taulelle, F.; Férey, G. *Angew. Chem., Int. Ed.* **2006**, *45*, 5974−5978.
(7) Cho, W.; Lee, Y. H.; Lee, H. J.; Oh, M. *Adv. Mater.* **2011**, *23*, 1720−1723.
(8) Jo, C.; Lee, H. J.; Oh, M. *Adv. Mater.* **2011**, *23*, 1716−1719.
(9) Zhang, X.; Dong, C.; Zapien, A.; Ismathullakhan, S.; Kang, Z.; Jie, J.; Zhang, X.; Chang, J. C.; Lee, C.-S.; Lee, S.-T. *Angew. Chem., Int. Ed.* **2009**, *48*, 1−4.
(10) Lu, W.; Chui, S. S.-Y.; Ng, K.-M.; Che, C. M. *Angew. Chem., Int. Ed.* **2008**, *47*, 4568−4572.
(11) Chifotides, H. T.; Dunbar, K. R. *Acc. Chem. Res.* **2005**, *38*, 146−156.
(12) Karlin, K. D.; Tyeklar, Z. *Bioinorganic Chemistry of Copper*; Chapman & Hill: New York, 1993.
(13) Etcheverry, S. B.; Di Virgilio, A. L.; Nascimento, O. R.; Williams, P. A. M. *J. Inorg. Biochem.* **2012**, *107*, 25−33.
(14) Horcajada, P.; Chalati, T.; Serre, C.; Gillet, B.; Sebrie, C.; Baati, T.; Eubank, J. T.; Heurtaux, D.; Clayette, P.; Kreuz, C.; Chang, J.-S.; Hwang, Y. K.; Marsaud, V.; Bories, P.-N.; Cynober, L.; Gil, S.; Férey, G.; Couvreur, P.; Gref, R. *Nat. Mater.* **2010**, *9*, 172−178.
(15) (a) Rocca, J. D; Liu, D.; Lin, W. *Acc. Chem. Res.* **20011**, *44*, 957−968. (b) Gao, Q.; Jiang, F. L.; Wu, M. Y.; Huang, Y. G.; Wei, W.; Hong, M. C. *Cryst. Growth Des.* **2010**, *10*, 184−190. (c) Yaghi, O. M.; O'Keeffe, M.; Ockwig, N. W.; Chae, H. K.; Eddaoudi, M.; Kim, J. *Nature* **2003**, *423*, 705−714. (d) Eddaoudi, M.; Kim, J.; Rosi, N.; Vodka, D.; Wachter, J.; O'Keeffe, M.; Yaghi, O. M. *Science* **2002**, *295*, 469−472. (e) Ma, J.; Jiang, F. L.; Chen, L.; Wu, M. Y.; Zhang, S. Q.; Han, D.; Feng, R.; Hong, M. C. *Cryst. Growth Des.* **2011**, *11*, 3273−3281.
(16) (a) Ni, Z.; Masel, R. I. *J. Am. Chem. Soc.* **2006**, *128*, 12394−12395. (b) Rieter, W. J.; Taylor, K. M. L.; An, H.; Lin, W.; Lin, W. *J. Am. Chem. Soc.* **2006**, *128*, 9024−9025. (c) Liu, K.; You, H.; Jia, G.; Zheng, Y.; Huang, Y.; Song, Y.; Yang, M.; Zhang, L.; Zhang, H. *Cryst. Growth Des.* **2010**, *10*, 790−797. (d) Dang, S.; Liu, Q.; Liu, K.; Guo, Z.; Sun, L.; Song, S.; Zhang, H. *Cryst. Growth Des.* **2010**, *10*, 4662−4667. (e) Jeon, Y.-M.; Armatas, G. S.; Heo, J.; Kanatzidis, M. G.; Mirkin, C. A. *Adv. Mater.* **2008**, *20*, 2105−2110.
(17) (a) Jeon, Y.-M.; Armatas, G. S.; Kim, D.; Kanatzidis, M. G.; Mirkin, C. A. *Small* **2009**, *5*, 46−50. (b) Jung, S.; Oh, M. *Angew. Chem., Int. Ed.* **2008**, *47*, 2049−2051. (c) Liu, X. *Angew. Chem., Int. Ed.* **2009**, *48*, 2−6. (d) Spokoyny, A. M.; Kim, D.; Sumrein, A.; Mirkin, C. A. *Chem. Soc. Rev.* **2009**, *38*, 1218−1227.
(18) Carné, A.; Carbonell, C.; Imaz, I.; Maspoch, D. *Chem. Soc. Rev.* **2011**, *40*, 291−305.
(19) Imaz, I.; Hernando, J.; Ruiz-Molina, D.; Maspoch, D. *Angew. Chem., Int. Ed.* **2009**, *48*, 2325−2329.
(20) Wang, K. B.; Geng, Z. R.; Yin, Y. X.; Ma, X. Y.; Wang, Z. L. *CrystEngComm* **2011**, *13*, 5100−5104.
(21) Dikusar, E. A.; Potkin, V. I.; Kozlov, N. G.; Yuvchenko, A. P. *Russ. J Gen. Chem.* **2009**, *79*, 258−263.
(22) Lee, H. J.; Cho, W.; Oh, M. *CrystEngComm* **2010**, *12*, 3959−3963.
(23) Diring, S.; Furukawa, S.; Takashima, Y.; Tsuruoka, T.; Kitagawa, S. *Chem. Mater.* **2010**, *22*, 4531−4538.
(24) Farha, O. K.; Spokoyny, Y. M.; Mulfort, K. L.; Galli, S.; Hupp, J. T.; Mirkin, C. A. *Small* **2009**, *5*, 1727−1731.
(25) Wang, X.; Guerzo, A. D.; Schmehl, R. H. *ChemComm.* **2002**, 2344−2345.
(26) Wang, K. B.; Yin, Y. X.; Li, C. Y.; Geng, Z. R.; Wang, Z. L. *CrystEngComm* **2011**, *13*, 6231−6236.
(27) Viuelas-Zahnos, E.; Luna-Giles, F.; Torres-Garca, P.; Fernndez-Caldern, M. C. *Eur. J. Med. Chem.* **2011**, *46*, 150−159.
(28) Prathima, B.; Rao, Y. S.; Reddy, S. A.; Reddy, Y. P.; Reddy, A. V. *Spectrochim. Acta A* **2010**, *77*, 248−252.
(29) Kumar, G.; Kumar, D.; Devi, S.; Johari, R.; Singh, C. P. *Eur. J. Med. Chem.* **2010**, *45*, 3056−3062.
(30) Zanella, A.; Gandin, V.; Porchia, M.; Refosco, F.; Tisato, F.; Sorrentino, F.; Scutari, G.; Rigobello, M. P.; Marzano, C. *Invest. New Drugs* **2011**, *29*, 1213−1223.